

ELECTRONIC SUPPLEMENTARY INFORMATION

Passive control of cell locomotion using micropatterns: the effect of micropattern geometry on the migratory behavior of adherent cells

Sang-Hee Yoon,^{abc} Young Kyun Kim,^{ad} Eui Don Han,^e Young-Ho Seo,^e Byeong Hee Kim,^e and Mohammad R. K. Mofrad^{*a}

^a Department of Bioengineering, University of California, Berkeley, California 94720, USA.

^b Department of Mechanical Engineering, University of California, Berkeley, California 94720, USA.

^c Wyss Institute for Biologically Inspired Engineering, Harvard University, Cambridge, Massachusetts 02138, USA.

^d Molecular Environmental Biology, University of California, Berkeley, California 94720, USA.

^e Medical and Bio-Material Research Center, Kangwon National University, Chuncheon 200-701, Republic of Korea.

* To whom correspondence should be addressed. Mailing address: 208A Stanley Hall, University of California, Berkeley, CA 94720, USA; E-mail: mofrad@berkeley.edu; Fax: +1-510-642-5835; Tel: +1-510-642-8165

Optical time-sequential image of cell migration

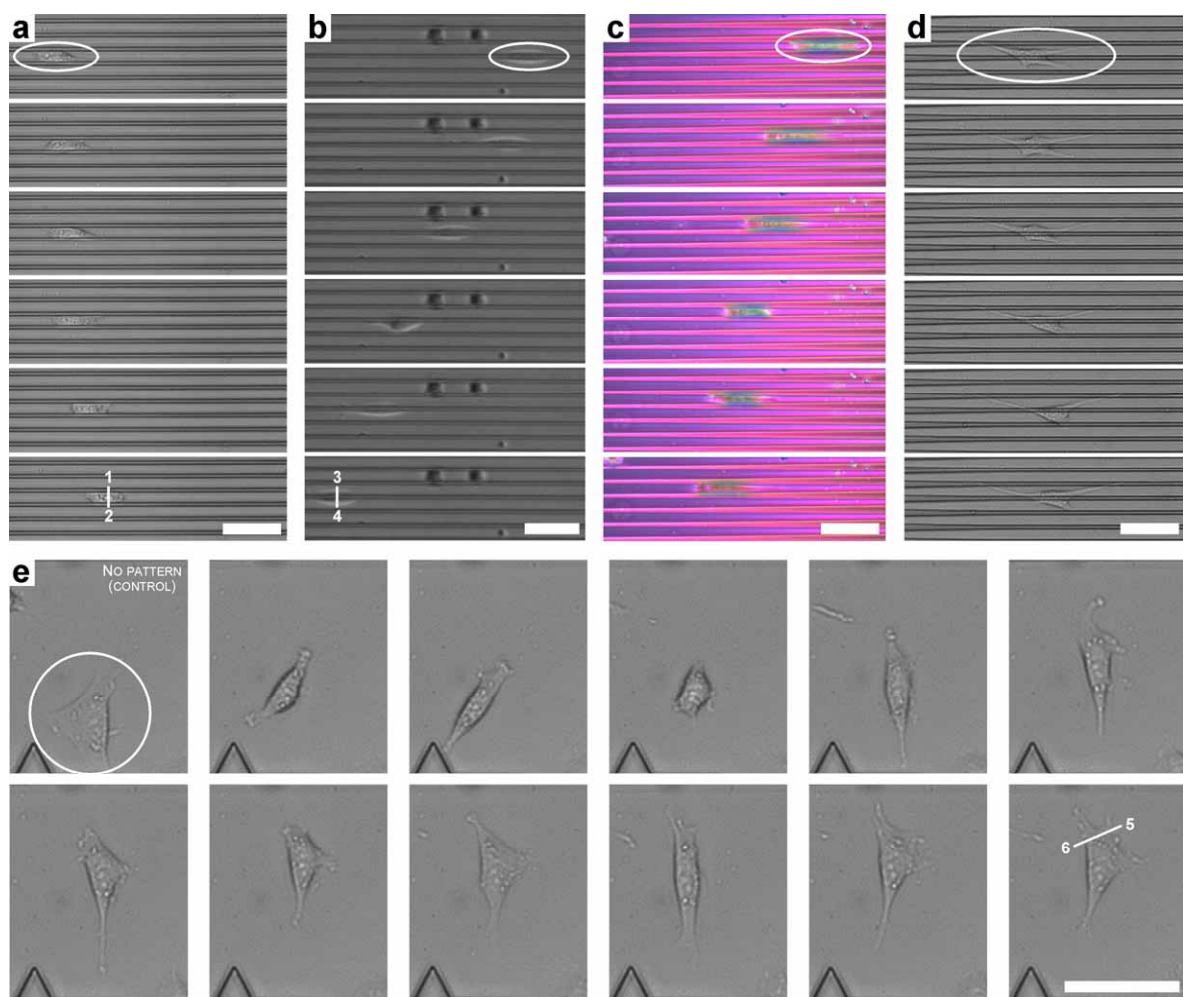


Fig. S1 Optical time-sequential images of NIH 3T3 fibroblasts moving on the Rome platform. (a) Cell migration along the single trough of micropatterns having a width of 10 μm (zone III). (b) Cell migration along the single trough of micropatterns having a width of 3 μm (zone I). (c) Cell migration along the single trough of micropatterns having a divergence angle of 1° (zone II). (d) Cell migration along the multiple (more than two) troughs (or ridges) of micropatterns having a width of 3 μm . (e) Unguided cell migration on a flat substrate with no topographical feature (control group 2). All images of (a-e) are taken every half hour after 24 hours of cell seeding. Scale bars of (a-e) are 50 μm .

Biocompatibility characterization of ORMOCOMP (cell proliferation rate)

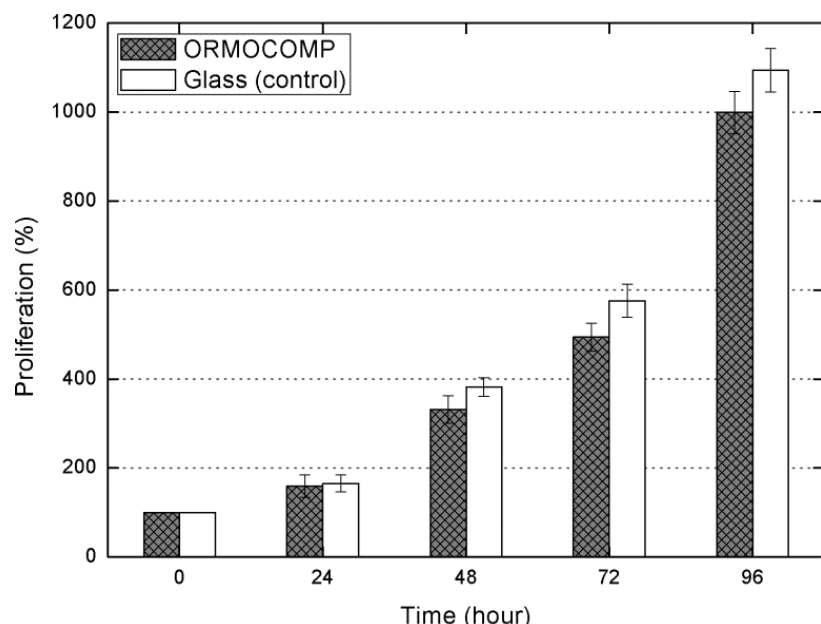


Fig. S2 Growth behavior of NIH 3T3 fibroblasts cultivated on a coverslip coated with the ORMOCOMP resin, compared to that of the cells cultivated on a glass coverslip. The presence of the ORMOCOMP resin does not significantly alter cell growth (and cell adhesion), thus verifying the biocompatibility of the ORMOCOMP resin.

Biocompatibility characterization of ORMOCOMP (cell morphology)

The biocompatibility of a UV-curable resin, ORMOCOMP, was additionally characterized by inspecting cell morphology thereon as well as using a live/dead viability kit (Invitrogen). The detailed experimental protocol used here was the same as that described in our previous research.⁴⁸ Two groups of NIH 3T3 fibroblasts were seeded on two substrates (a coverslip coated with the ORMOCOMP resin and a glass coverslip made of borosilicate glass (control group 1, Ted Pella, Inc.)). The cells were cultured on each substrate for 24 hours and then their morphology and viability were observed. The morphology and viability of the cells cultivated on the coverslip coated with the ORMOCOMP resin were almost same as those of the cells cultivated on the glass coverslip (**Fig. S3**). In other words, the presence of the ORMOCOMP resin did not significantly alter the morphology and viability of the cells, thus verifying the biocompatibility of the ORMOCOMP resin.

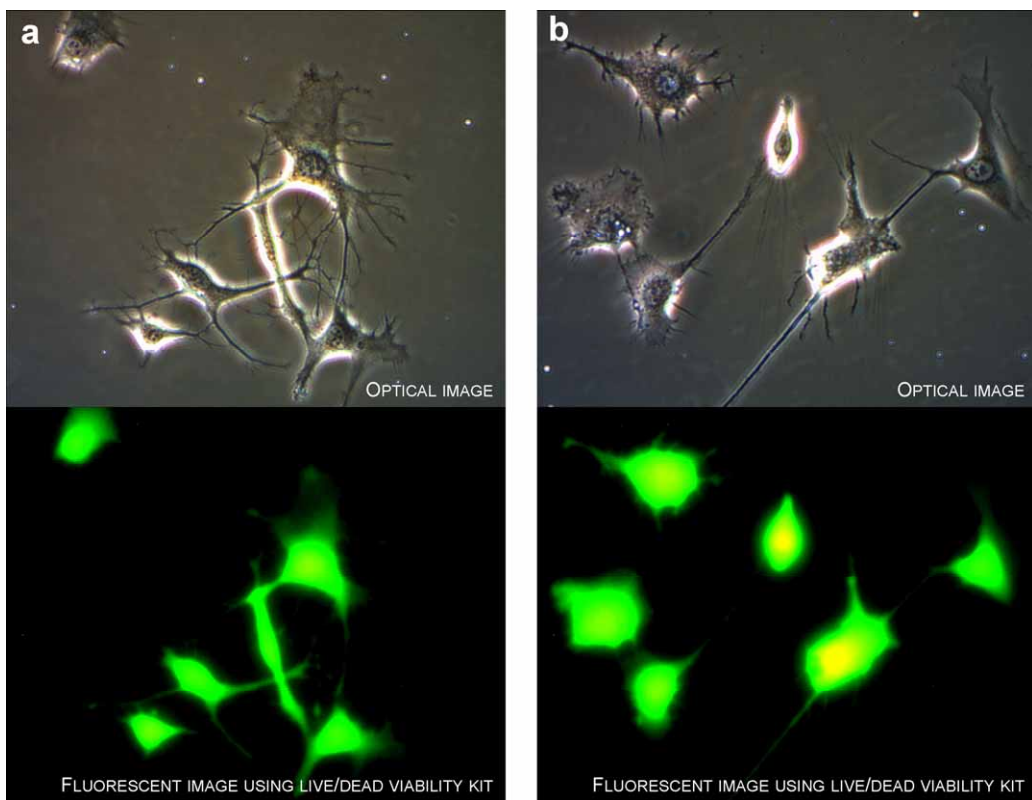


Fig. S3 Biocompatibility characterization of the ORMOCOMP resin using a live/dead viability kit. (a) Optical (top) and fluorescent (bottom) images of NIH 3T3 fibroblasts cultivated on the coverslip coated with the ORMOCOMP resin. (b) Optical and fluorescent images of the cells cultivated on a glass coverslip. The presence of the ORMOCOMP resin does not change the morphology and viability of the cells noticeably.

Cell biology analysis of cell migration controlled by diverging micropatterns

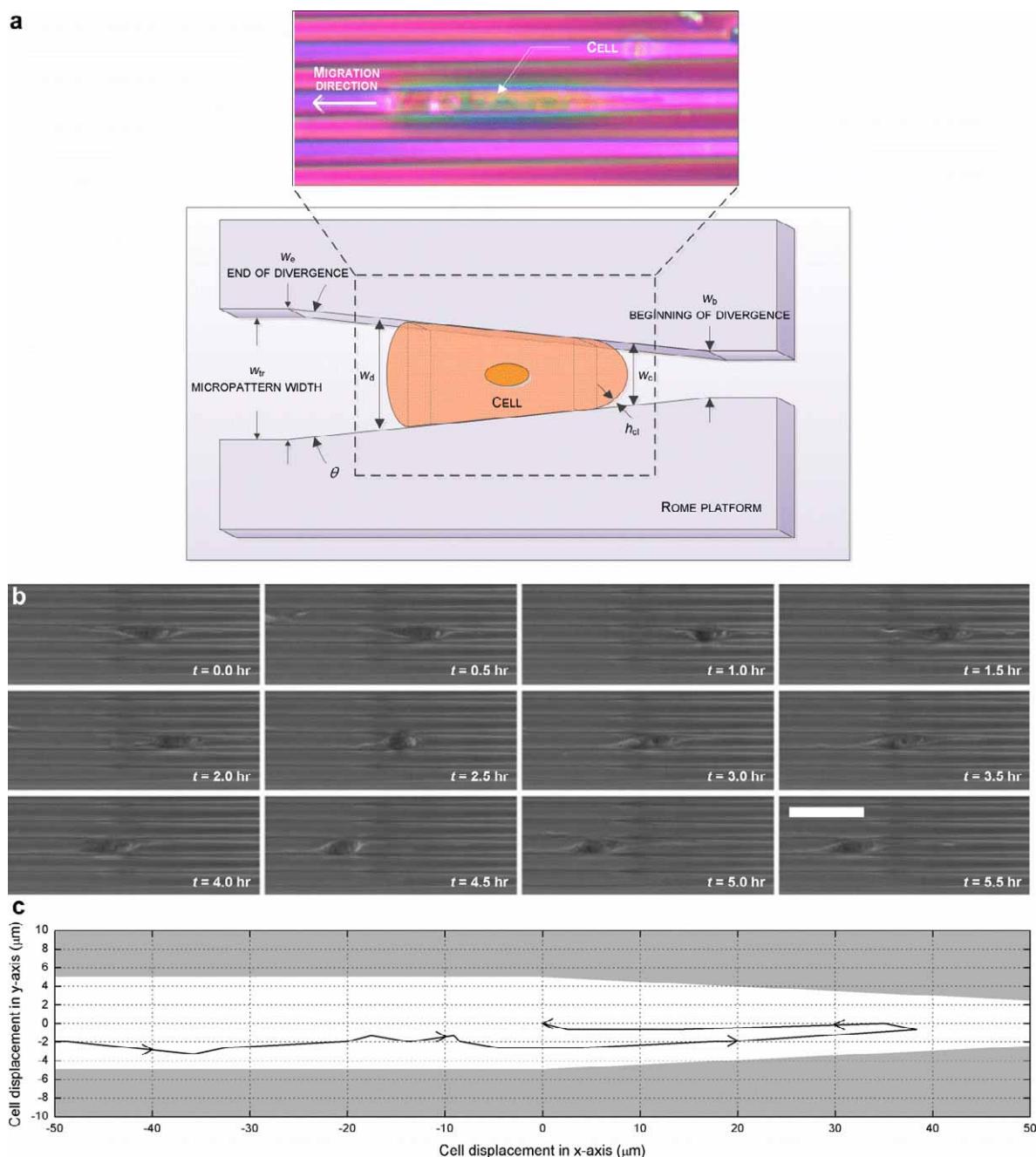


Fig. S4 One-directional cell migration controlled by the Rome platform. (a) Cell migration guided by diverging micropatterns. An adherent cell changes its morphological shape along the diverging micropatterns; the change in cell morphology makes the cell migrate in a diverging direction of the micropatterns. (b) Optical time-sequential images showing cell migration on the diverging micropatterns. Even when a cell starts to migrate in the opposite direction (converging direction of the micropatterns), the diverging micropatterns compel the cell to move in the diverging direction. (c) Cell migration path determined from the optical time-sequential images of (b). Scale bar of (b) is 50 μm .

Fluid mechanics analysis of cell migration controlled by diverging micropatterns

Fluid mechanics analysis was also made to explain how micropatterns having a divergence angle (called “diverging micropatterns”) controlled the migration direction of adherent cells (NIH 3T3 fibroblasts). From a fluid mechanics viewpoint, the cell migration guided by diverging micropatterns was assumed as a viscous flow in a rectangular microchannel having a channel length of l_{ch} , a width of w_{ch} , and a height of h_{ch} . The flow resistance in the microchannel, \mathcal{Q}_{ch} , can be expressed as,

$$\mathcal{Q}_{\text{ch}} = \frac{12\eta l_{\text{ch}}}{h_{\text{ch}}^3 w_{\text{ch}}} \left\{ 1 - \sum_{n=1,3,5,\dots}^{\infty} \frac{1}{n^5} \frac{192}{\pi^5} \frac{h_{\text{ch}}}{w_{\text{ch}}} \tanh\left(\frac{n\pi w_{\text{ch}}}{2h_{\text{ch}}}\right) \right\}^{-1}, \quad (\text{S1})$$

where η is a fluid viscosity.⁵⁰ The ratio of fluidic resistance in a diverging direction of the micropatterns to that in a converging direction, $\mathcal{Q}_{\text{d}} / \mathcal{Q}_{\text{c}}$, can be written as,

$$\frac{\mathcal{Q}_{\text{d}}}{\mathcal{Q}_{\text{c}}} = \frac{w_{\text{c}}}{w_{\text{d}}} \left\{ \frac{1 - \sum_{n=1,3,5,\dots}^{\infty} \frac{1}{n^5} \frac{192}{\pi^5} \frac{h_{\text{cl}}}{w_{\text{c}}} \tanh\left(\frac{n\pi w_{\text{c}}}{2h_{\text{cl}}}\right)}{1 - \sum_{n=1,3,5,\dots}^{\infty} \frac{1}{n^5} \frac{192}{\pi^5} \frac{h_{\text{cl}}}{w_{\text{d}}} \tanh\left(\frac{n\pi w_{\text{d}}}{2h_{\text{cl}}}\right)} \right\} \approx \frac{w_{\text{c}}}{w_{\text{d}}} < 1, \quad (\text{S2})$$

where w_{c} and w_{d} are the widths of the leading and trailing edges of the cell having a height of h_{cl} , respectively (**Fig. S3a**). The calculated ratio of fluidic resistance was less than 1, meaning cell migration in a diverging direction had less energy loss caused by fluidic resistors than that in a converging direction. Adherent cells migrating on a diverging micropattern therefore moved in a diverging direction of the micropatterns, rather than in a converging direction.

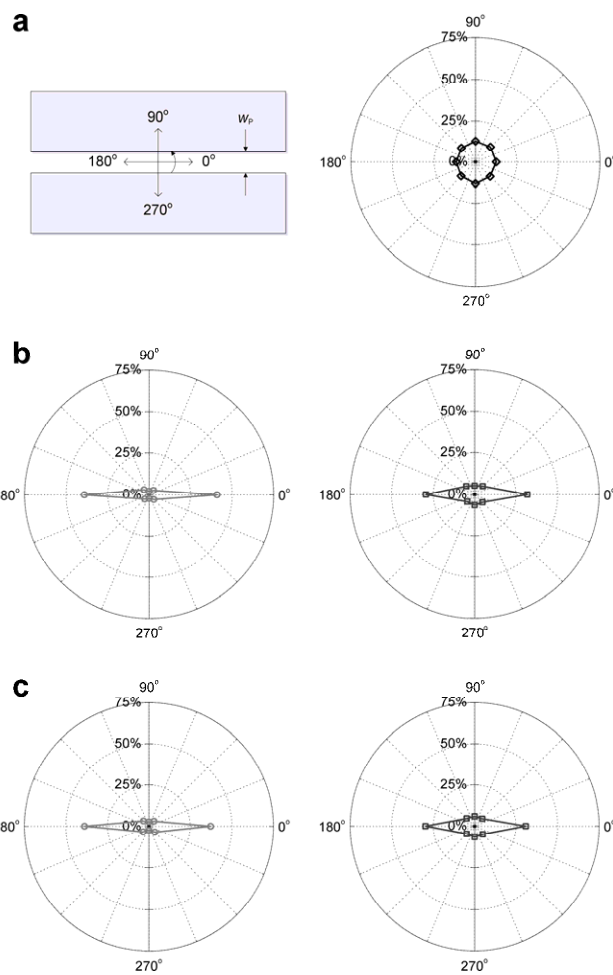


Fig. S5 Angular distribution of cell migration direction induced by micropatterns having different widths, showing the percentage of the cells that migrate along each 45-degree angular sector (e.g., $0\pm22.5^\circ$, $45\pm22.5^\circ$, $90\pm22.5^\circ$, etc.). The sector with a higher angular distribution value indicates that more cells move in the direction of the sector. (a) On a control group 2 (a flat substrate made of the ORMOCOMP resin, right) with an angle notation (left). (b) On the troughs (left) and ridges (right) of the micropatterns having a width of 3 μm . (c) On the troughs (left) and ridges (right) of the micropatterns having a width of 10 μm . The detailed experimental data are summarized in **Table S2**.

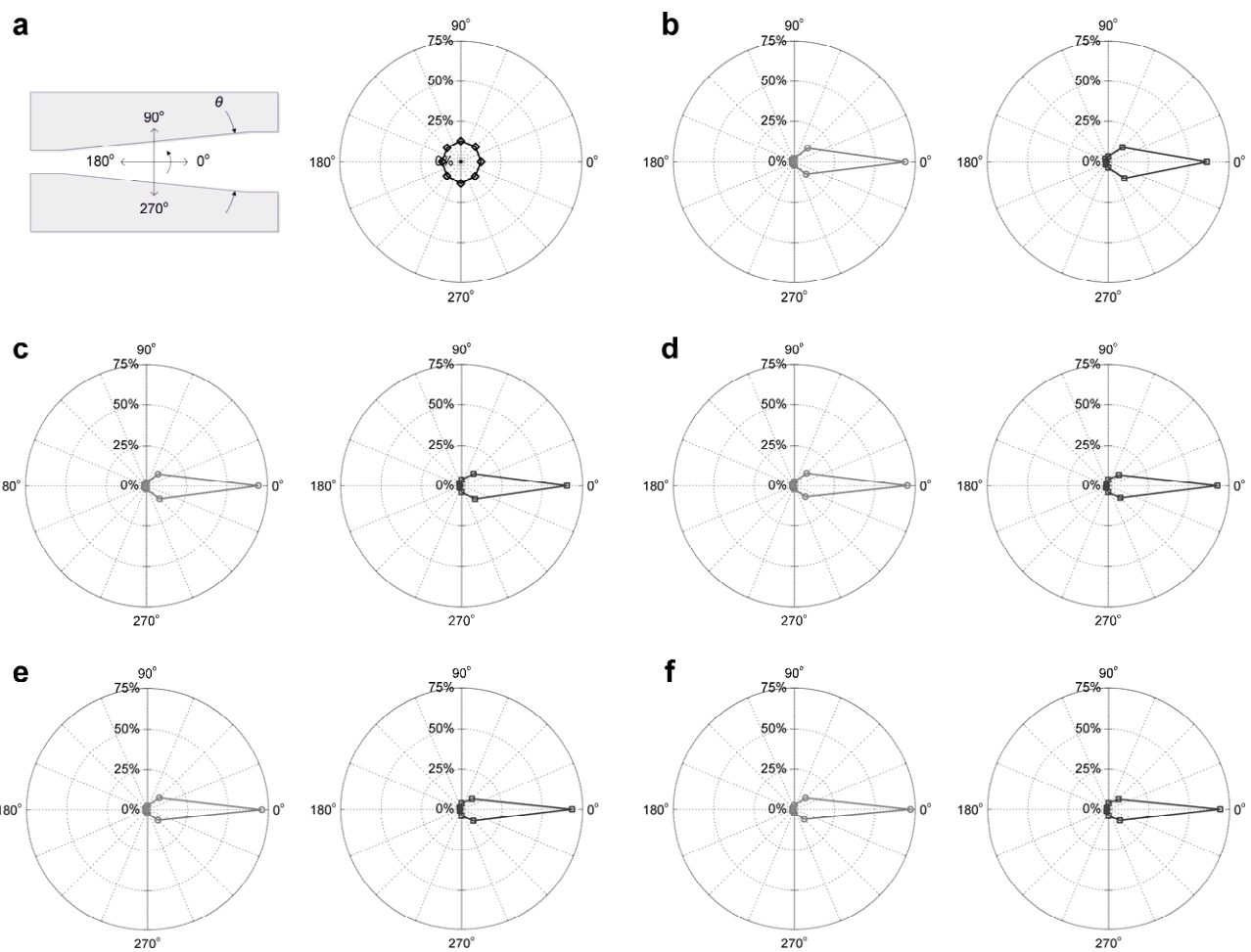


Fig. S6 Angular distribution of cell migration direction induced by micropatterns having different divergence angles of 0.5 to 5.0°, showing the percentage of the cells that migrate along each 45-degree angular sector (e.g., e.g., $0\pm22.5^\circ$, $45\pm22.5^\circ$, $90\pm22.5^\circ$, etc.). (a) On a control group 2 (a flat substrate made of the ORMOCOMP resin, right) with an angle notation (left). (b) On the troughs (left) and ridges (right) of the micropatterns having a divergence angle of 0.5°. (c) On the troughs (left) and ridges (right) of the micropatterns having a divergence angle of 1.0°. (d) On the troughs (left) and ridges (right) of the micropatterns having a divergence angle of 2.0°. (e) On the troughs (left) and ridges (right) of the micropatterns having a divergence angle of 4.0°. (f) On the troughs (left) and ridges (right) of the micropatterns having a divergence angle of 5.0°. The detailed experimental data are summarized in **Table S2**.

Table S1 Effect of the geometry of micropatterns on cell location, showing that cell location is controllable by changing physical cues (i.e., micropatterns). Among the cells located on each region, the number of NIH 3T3 fibroblasts located on the ridges of micropatterns is compared to that of the cells located on the troughs. More cells are located on the troughs than on the ridges, and the intensity of this tendency is proportional not to the divergence angle of micropatterns but to the average width of micropatterns.

Pattern	Avg. pattern width (μm)	Divergence angle (degree)	Zone ¹		Percentage ² (%)
Parallel	3.0	0.0	III	+	29.23 \pm 2.06
			I	-	70.77 \pm 2.06
	10.0	0.0	I	+	40.62 \pm 3.17
			III	-	59.38 \pm 3.17
Diverging	6.5 (= (3+10)/2)	0.5	II	+	36.24 \pm 3.08
			II	-	63.76 \pm 3.08
	1.0		II	+	37.33 \pm 2.82
			II	-	62.67 \pm 2.82
	2.0		II	+	36.77 \pm 2.95
			II	-	63.23 \pm 2.95
	4.0		II	+	35.15 \pm 3.16
			II	-	64.85 \pm 3.16
	5.0		II	+	37.71 \pm 5.57
			II	-	62.29 \pm 5.57

¹ “+” indicates the ridge of micropatterns and “-” means the trough of micropatterns (see Fig.1b).

² All data are represented as mean \pm standard error (of the mean), obtained from at least 10 independent experiments.

Table S2 Effect of the geometry of micropatterns on cell migration, showing that cell migration is controlled by creating the gradient of physical cues (i.e., divergence angle) whereas the other migratory characteristics are affected by adjusting the amount of them (i.e., micropattern width). Among the cells moving on each region, the number of NIH 3T3 fibroblasts migrating along the micropatterns is compared to that of the cells travelling across them. Moreover, the migratory behavior of the cells migrating on the micropatterns is quantified in terms of cell migration speed, directional persistence time, and random motility coefficient.

Pattern	Avg. pattern width (μm)	Divergence angle (degree)	Zone	Migration along micropatterns ¹ (%)	Migration across micropatterns ² (%)	Cell migration speed ($\mu\text{m}/\text{min}$)	Dir. persistence Time (minute)	Random motility Coefficient ($\mu\text{m}^2/\text{min}$)
Parallel	3.0	0.0	III +	61.19 \pm 4.91	11.77 \pm 4.38	0.69 \pm 0.05	47.76 \pm 20.37	11.37 \pm 3.84
		—	I —	79.83 \pm 4.32	4.40 \pm 2.28	0.76 \pm 0.04	61.45 \pm 25.11	17.75 \pm 5.13
	10.0	0.0	I +	60.34 \pm 2.61	12.62 \pm 3.95	0.31 \pm 0.03	106.31 \pm 21.34	5.11 \pm 0.93
		—	III —	75.85 \pm 3.27	5.21 \pm 1.81	0.34 \pm 0.02	129.55 \pm 37.06	7.49 \pm 1.83
Diverging	6.5	0.5	II +	66.46 \pm 3.41	6.47 \pm 3.92	0.55 \pm 0.02	53.67 \pm 22.51	8.12 \pm 3.06
		—	II —	74.83 \pm 3.11	4.05 \pm 2.16	0.57 \pm 0.02	79.32 \pm 18.67	12.89 \pm 2.15
	1.0	II +	70.95 \pm 2.54	7.62 \pm 3.19	0.54 \pm 0.02	66.69 \pm 19.67	9.72 \pm 2.86	
		—	II —	75.42 \pm 2.79	4.12 \pm 1.92	0.56 \pm 0.02	82.52 \pm 25.16	12.94 \pm 2.95
	2.0	II +	73.62 \pm 3.27	7.83 \pm 3.15	0.57 \pm 0.02	70.85 \pm 19.81	11.51 \pm 2.98	
		—	II —	76.21 \pm 4.21	4.78 \pm 2.92	0.57 \pm 0.02	83.46 \pm 19.16	13.55 \pm 2.95
	4.0	II +	74.37 \pm 3.81	7.92 \pm 4.31	0.53 \pm 0.03	82.27 \pm 20.24	11.55 \pm 2.67	
		—	II —	77.11 \pm 2.54	4.99 \pm 1.07	0.51 \pm 0.02	104.95 \pm 21.95	13.64 \pm 2.88
	5.0	II +	75.22 \pm 2.61	7.96 \pm 2.77	0.53 \pm 0.03	99.64 \pm 19.54	13.99 \pm 2.13	
		—	II —	78.36 \pm 4.32	5.11 \pm 1.78	0.52 \pm 0.02	105.34 \pm 18.95	14.24 \pm 2.44
Control 2 ³	∞	—	—	24.09 \pm 1.90	25.88 \pm 1.24	0.26 \pm 0.02	40.71 \pm 14.62	1.38 \pm 0.52

¹ The percentage of the cells that migrate along two 45-degree angular sectors of $0\pm22.5^\circ$ and $180\pm22.5^\circ$ where 0° is a direction of the micropatterns (or positive x -axis direction, see Figs. S5a and S6a).

² The percentage of the cells that travel along two 45-degree angular sectors of $90\pm22.5^\circ$ and $270\pm22.5^\circ$.

³ A control group is a flat substrate made of the ORMOCOMP resin.

Videos of cell migration along different micropatterns

All videos are created by recording the time-sequential images taken every half hour at a rate of 2 frames per second.

- Video S1.** Cell migration along the single trough of the micropatterns having a width of 10 μm .
- Video S2.** Cell migration along the single trough of the micropatterns having a width of 3 μm .
- Video S3.** Cell migration along the single trough of the micropatterns having a divergence angle of 1°.
- Video S4.** Cell migration along the multiple (more than two) troughs (or ridges) of the micropatterns having a width of 3 μm .
- Video S5.** Unguided cell migration on a flat substrate with no topographical feature made of the ORMOCOMP resin (control group 2).